Associative polymers bearing *n*-alkyl hydrophobes: Rheological evidence for microgel-like behavior

Robert J. English

Department of Color Chemistry, The University of Leeds, Leeds LS2 9JT, United Kingdom

Srinivasa R. Raghavan

Department of Chemical Engineering, North Carolina State University, Raleigh, North Carolina 27695-7905

Richard D. Jenkins

Technical Center, Union Carbide Asia Pacific Inc., 16 Science Park Drive, The Pasteur, Singapore 118227

Saad A. Khan[a)]

Department of Chemical Engineering, North Carolina State University, Raleigh, North Carolina 27695-7905

(Received 9 December 1998; final revision received 2 June 1999)

Synopsis

Rheological techniques are used to probe the behavior of hydrophobic alkali-swellable emulsion (HASE) polymers, bearing *n*-alkyl hydrophobes, in aqueous alkaline media. The polymers possess a comb-like architecture with a polyelectrolyte backbone (ethyl acrylate-*co*-methacrylic acid) and hydrophobes ($\sim$ 16 per polymer chain) tethered to the backbone via polyether side chains. The size of the hydrophobes is varied from *n*-C_8 to *n*-C_{20} in this study. It is shown that, at such a level of hydrophobic modification, and at relatively high polymer concentrations, the microstructure in these polymer systems is akin to that existing in concentrated microgels. Thus, the original polymer latex particles swell extensively in alkaline media and disintegrate to form a system of close-packed, compressible (''soft'') aggregates. This is reflected in the rheological response of the system where we observe a high steady shear viscosity with no zero-shear plateau at low shear rates followed by considerable shear thinning and, a characteristic power-law behavior ($G', G'' \sim \omega^{0.4}$) under oscillatory shear persisting over a broad range of time scales. Concentration-independent master curves are obtained for the storage modulus, G', with the level of G' increasing with hydrophobe size. The similarity in the dynamic response suggests that there exists a qualitative equivalence in microstructure over the range of systems, the only difference being the ''softness'' or compressibility of the particles. Data from this study are also contrasted with those for a similar HASE polymer bearing a smaller number of alkylaryl hydrophobes [English *et al.*, J. Rheol. **41**, 427–444 (1997)]. In the latter case, the rheology can be interpreted in terms of hydrophobic

[a)]Author to whom all correspondence should be addressed;
Phone: (919) 515-4519; Fax: (919) 515-3465; electronic mail: khan@eos.ncsu.edu

associations and chain entanglements occurring in solution. Thus, subtle variations in molecular architecture are shown to cause significant differences in morphology and microstructure for these polymer systems. © *1999 The Society of Rheology.* [S0148-6055(99)00505-2]

I. INTRODUCTION

Current industrial practice favors the use of hydrophobic alkali-swellable emulsion (HASE) polymers as rheology modifiers in water-borne paints and coatings [Shay and Rich (1986); Shay (1989)]. These materials offer an alternative to technologies based on nonionic associative polymer systems [the latter are commonly denoted as hydrophobic ethoxylated urethane (HEUR) polymers]. In contrast to HEUR polymers, where the majority of recent experimental and theoretical considerations have been focussed [Annable *et al.* (1993); Groot and Agterof (1995); Semenov *et al.* (1995); Xu *et al.* (1996); Tam *et al.* (1998)], there have been few comprehensive studies on the rheological properties of HASE polymers. Correspondingly, less emphasis has been placed on developing suitable theoretical approaches for describing the solution properties of hydrophobically modified polyelectrolytes. Borisov and Halperin (1995, 1996a, b) have recently made a significant contribution, however, in considering the association of ''polysoaps,'' i.e., water-soluble polymers bearing numerous hydrophobic segments. There has also been recent theoretical and experimental interest in hydrophobically modified polymers that exhibit thermal gelation [Bromberg (1998); Rubinstein and Semenov (1998)]. A useful summary of the solution behavior of polymers bearing associative groups has been provided by Rubinstein and Dobrynin (1997).

In a previous study, we presented rheological data for a novel HASE polymer bearing a small number of complex alkylaryl hydrophobes of high molar volume [English *et al.* (1997)]. The rheology of this material was shown to be notably more complex than that of the HEUR systems. In the case of HEUR polymers, the rheology has been widely shown to conform to a simple Maxwell model under oscillatory shear, with stress relaxation in these systems being controlled purely by the disengagement rate of hydrophobes from their junction domains [Jenkins (1990); Jenkins *et al.* (1991); Tanaka and Edwards (1992); Annable *et al.* (1993)]. In contrast, we postulated that the dissipation of stress in HASE systems is moderated by the coexistence of hydrophobic associations and topological entanglements so that one can evoke, qualitatively, the concepts of ''hindered reptation'' put forward by Liebler and co-workers (1991). Perhaps the most striking effect of the placement of a small number of large hydrophobes onto the HASE polymer was the occurrence of shear-induced structuring at lower polymer concentrations. We noted this phenomenon under steady shear, large amplitude oscillatory shear and parallel superposed steady/dynamic shear. From a microstructural viewpoint, we attributed these effects to the formation of intermolecular associations, at the expense of intramolecular associations accompanying the coil stretch transition during shear. The competition between intra- and intermolecular associations has similarly been noted in other studies on hydrophobically modified polyectrolytes [Branham *et al.* (1996)].

In our ongoing studies on HASE systems, our goal is to ascertain the key structure–property relationships controlling the performance of these polymers in aqueous media. Explicit knowledge of this kind will facilitate the design of new products with improved or specifically tailored application properties. We have therefore explored possible variations in the molecular constitution of these polymers, particularly with a view to elucidate the ''associative'' interactions between hydrophobes and the attendant microstructures produced. The molecular architecture of HASE polymers tends to follow a common theme, but as will be seen, there is considerable latitude for variation [Jenkins *et al.*

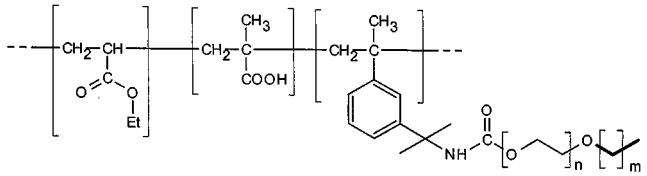

FIG. 1. Chemical constitution of HASE polymers bearing *n*-alkyl hydrophobes.

(1994, 1996)]. Commonly, a comb-like architecture is favored, with the hydrophobes situated on poly(oxyethylene) side chains, distributed randomly along a polyelectrolyte backbone. These side chains are introduced by means of a copolymerizable urethane-functional macromer, bearing the hydrophobe at one end and an unsaturated group at the other. The number of hydrophobes per chain is readily tailored by varying the proportion of macromer in the emulsion polymerization recipe, while the length of the side chains is manipulated by varying the molecular weight of the poly(oxyethylene) segment. Hydrophobes may be selected from alkyl, alkylaryl, or even complex poly(alkylaryl) moieties [Jenkins *et al.* (1991)].

In the present study, we are especially interested in the effect of hydrophobe size. In order to allow precise control of hydrophobe constitution, we employ macromers derived from the ethoxylation of analytically pure samples of *n*-alkanols. These macromers are used to prepare a series of HASE polymers of similar constitution, varying only in the size of the hydrophobe (n-C_8,n-C_{16},n-C_{20}). We then examine the rheology of these polymers on swelling/solubilization in an aqueous medium. Data obtained in the present study will also be contrasted with that from our previously published study [English *et al.* (1997)], where the polymer contained a smaller number of relatively large hydrophobic groups. The HASE polymers considered here are identical to those recently studied by Tirtaatmadja *et al.* (1997a, b) and Kumacheva *et al.* (1997). Our study is a much more extensive investigation of the rheology of these systems, spanning a range of polymer concentrations. More importantly, we offer an alternative interpretation of the rheological data, where we show our systems to be analogous to concentrated microgels rather than to polymer solutions.

II. EXPERIMENT

A. Preparation of HASE polymers

The HASE polymers were prepared via a procedure adapted from that disclosed previously [Jenkins *et al.* (1994)]. The idealized structure of the polymers is depicted in Fig. 1. The polymers are the emulsion polymerization product of methacrylic acid (MAA), ethyl acrylate (EA), and a macromer which bears the hydrophobic group. Polymer dispersions were prepared to have identical molar compositions in terms of the monomer feed composition employed. This was based on a ratio of 0.49/0.50/0.01 for MAA/EA/macromer. In terms of weight percent this corresponds to the approximate composition of 40/45/15 of the above monomers, respectively. A control polymer based on MAA/EA, but with no hydrophobic modification, was also prepared.

As we vary the type of macromer, we assume that the number of hydrophobes per chain, the monomer sequence distribution and molecular weight of each of the polymers are similar, thus facilitating a study on the effects of variation in the size of the hydrophobic moiety. These assumptions have been verified in an independent study using size exclusion chromatography [Islam *et al.* (1997, 1999)]. Reliable fractionation of HASE

TABLE I. Characteristics of alkanol ethoxylate precursors and macromers.

Hydrophobe	Formula	*m*	Mn (OH, end group)	*n*	Macromer Calc. Mn
n-octyl	C_8H_{17}	7	1564	33	1765
n-hexadecyl	$C_{16}H_{33}$	15	1726	35	1962
n-eicosanyl	$C_{20}H_{41}$	19	1835	35	2036

polymers requires effective suppression of hydrophobic associations which tend to cause polymer aggregation. This has been achieved by both hydrolytic cleavage of the side chains from the polymer backbone and also by complexation of the hydrophobes with cyclodextrins. The molecular weights ($\bar{M}_w$) of the polymers bearing different *n*-alkyl hydrophobes was found to be similar at $\sim 2\times10^5$ Da—corresponding to around 16 hydrophobes per chain on average. The molecular weight of the control polymer was found to be somewhat different at $\sim 7\times10^5$ Da—the lower values for the *n*-alkyl modified polymers might arise due to the possibility of chain transfer to the macromer during their synthesis.

1. Synthesis of alkanol ethoxylate precursors

The *n*-alkanols viz *n*-octanol (C_8), *n*-hexadecanol (C_{16}) and *n*-eicosanol (C_{20}), were used without further purification ($\sim$ 99%). Each of the alkanols was ethoxylated in a pressure autoclave at 140 °C and 80 psi in the presence of a potassium hydroxide catalyst (0.25%, based on total reaction mass). Ethylene oxide sufficient to give a mean degree of ethoxylation of $\sim$ 35 was added in small aliquots, keeping the temperature and pressure constant throughout the reaction. On completion of the reaction, the ethoxylated products were poured hot from the reactor and allowed to solidify. Each alkanol ethoxylate was obtained as a waxy solid with only a slight amber coloration, and was characterized by means of end-group analysis (OH number) and size exclusion chromatography. The number average molecular weights of the ethoxylate precursors are summarized in Table I.

2. Synthesis of macromers

Macromers were prepared by reaction of the alkanol ethoxylates with the unsaturated isocyanate 3-isopropenyl-α,α-dimethylbenzyl isocyanate (*m*-TMI). The stoichiometric equivalent of the isocyanate was calculated based on the $\bar{M}_n$ of the alkanol ethoxylate determined by hydroxyl end-group analysis. The end-capping reaction was carried out in the melt at 85 °C, in the presence of a dibutyltin dilaurate catalyst (0.1% based on total reaction mass). On addition of the isocyanate to the ethoxylate melt and allowing the initial exotherm to subside, the reaction was allowed to proceed for 4 h in order to allow complete conversion. Each of the macromers was poured hot from the reactor and allowed to solidify, yielding a waxy solid. Size exclusion chromatography verified the absence of low molecular weight impurities and showed no change in the molecular weight distributions following end capping. The calculated molecular weights of the macromers, shown in Table I, are based on adding the formula weight of *m*-TMI isocyanate to the number average molecular weights of the alkanol ethoxylate precursors.

TABLE II. Compositions employed in the preparation of HASE polymer dispersions.

Polymer	Ref[a]	Hydrophobe	Molar composition MAA/EA/Macro	Weight fraction MAA/EA/Macro	Final solids content (wt %)
Control	RDJ31-1	None	0.49/0.51/-	45.00/55.00/-	30.82
C8	RDJ31-2	*n*-octyl	0.49/0.50/0.10	39.10/46.39/14.51	28.76
C16	RDJ31-4	*n*-hexadecyl	0.49/0.50/0.10	38.40/45.46/16.04	29.35
C20	RDJ31-5	*n*-eicosanyl	0.49/0.50/0.10	38.14/45.25/16.61	21.26

[a]See Tirtaatmadja *et al.* (1997a, 1997b).

3. Synthesis of HASE polymer

Monomer emulsions were prepared by blending monomers/macromer (proportions as in Table II, 620 g), Aerosol OT (75%, 26.0 g) and distilled, de-ionized water (60.0 g), by vigorous shaking in a sealed bottle. An initiator feed comprising sodium persulphate (8.0 g) and sodium bicarbonate (2.0 g) dissolved in distilled-de-ionized water (45.0 g) was also prepared. A 3 ℓ reactor was fitted with a four-blade stainless steel paddle stirrer, water condenser, nitrogen inlet and bubble trap, thermometer, monomer and initiator inlet tubes (1/8 in. Teflon), and immersed in a thermostated water bath. The reactor was charged with distilled, de-ionized water (1377 g), 2-sulphoethyl methacrylate (5.3 g) and Aerosol OT (75%, 5.3 g).

The monomer emulsion was charged to a 1 ℓ graduated feed cylinder and the initiator solution to a 100 cm^3 syringe pump. On heating the reactor to 80 °C under nitrogen, a proportion of the monomer emulsion (68 g) was introduced, together with the solution of sodium persulphate (16 g). Stirring was maintained for 30 min, allowing a seed latex to form, whereby the remaining monomer and initiator feeds were commenced at rates of 4.5 and 0.4 $cm^3\,min^{-1}$, respectively. On cessation of the initiator feed, the reaction was allowed to proceed for a further 1 h, prior to cooling to ambient temperature and filtration (200 mesh nylon sieve cloth). Each of the products was obtained as an opaque, milky white latex dispersion.

4. Preparation of HASE polymer solutions

The polymer dispersions were exhaustively dialyzed against distilled, de-ionized water prior to use (Spectrapore 7 cellulosic membrane, 50 000 Da cutoff), in order to remove serum electrolyte and excess anionic stabilizer. Samples for rheological characterization were prepared at concentrations between 5 and 40 gl^{-1}, depending on the presence and size of the hydrophobes. The latex dispersions were solubilized in the presence of 2-amino-2-methyl-1-propanol (AMP-95), at a level of 6.0×10^{-3} mol of the amine per gram of polymer (pH $\sim$ 9). Upon addition of the amine, the samples became visually transparent. Samples were prepared at constant ionic strength (0.05 M NaCl), by combining appropriate amounts of purified latex, distilled, de-ionized water, 0.5 M NaCl and 1.0 M AMP. Although HASE polymers are polyelectrolytes in their native state, the preparation protocol followed for this study eliminated/screened all polyelectrolyte or electrostatic effects [Guo *et al.* (1998); Tirtaatmadja *et al.* (1999)]. Following centrifugation to remove entrained air (2000 rpm, 15 min), each sample was allowed to stand for several days prior to characterization. Samples for dilute solution viscometry were prepared from a stock solution ($\sim$ 2 gl^{-1}), dialyzed against 0.05 M NaCl. Dilutions were made with the dialyzate, in order to eliminate errors in the measured intrinsic viscosities arising from thermodynamic effects.

B. Rheological characterization

Steady shear, dynamic and superposed steady/dynamic studies were carried out on a rheometrics dynamic stress rheometer, fitted with appropriate cone and plate and couette geometries. All rheometrical experiments were conducted at $25 \pm 0.1\,^{\circ}\mathrm{C}$. Drying out of the samples was prevented by coating any exposed surface with a low viscosity polydimethylsiloxane (PDMS) fluid (Dow Corning 200 Series, 10 cst). Intrinsic viscosities $[\eta]$ of each of the samples was measured at 25 °C using an Ubblehode capillary viscometer. Flow times were in excess of 600 s, eliminating the need to correct for kinetic energy effects.

As noted previously, the steady shear response of the HASE polymer samples was found to be influenced by the immediate shear history [English *et al.* (1997)]. In this respect, a preshearing regime was found necessary. Application of a steady shear stress, sufficient to generate a rate of deformation of approximately $5\ \mathrm{s}^{-1}$, was found appropriate in eliminating effects arising from the previous shear history of the polymer solutions. Preshearing was carried out for 180 s, followed by a rest period of 120 s prior to commencing the steady shear experiment. Steady shear data were collected using a step–stress procedure, with an equilibration time of 45 s being sufficient to allow the attainment of steady state in most cases, except at very low applied stresses. In the latter case, data were obtained from creep experiments, where the strain was directly monitored at a constant applied stress. Results obtained were verified on different geometries, in order to eliminate the existence of wall-slip effects. The maximum relative error in the steady shear and dynamic material functions was $\sim 5\%$.

In addition to conventional steady and dynamic oscillatory shear experiments, the response of selected samples to superposed steady/dynamic shear was also examined. The latter experiments were performed as previously described, again paying due regard to the avoidance of experimental errors [English *et al.* (1997); Tirtaatmadja *et al.* (1997a)]. This technique relies on the application of a harmonically varying stress, comprising the sum of a steady (mean) component σ_m and a dynamic component of amplitude σ_0 varying with angular frequency ω [Booij (1966); Ferry (1980)]:

$$\sigma(t) = \sigma_m + \sigma_0 \sin(\omega t). \tag{1}$$

The resultant deformation rate is also considered to comprise the sum of a steady component $\dot{\gamma}_m$ and a dynamic component of amplitude γ_0 such that

$$\dot{\gamma}(t) = \dot{\gamma}_m + \omega\gamma_0 \cos(\omega t - \delta). \tag{2}$$

Errors from instrument inertia were accounted for by ensuring that the measured steady shear functions ($\eta = \sigma_m / \dot{\gamma}_m$ or $\dot{\gamma}_m$) were constant across the range of angular frequencies employed. These data were further verified by comparison with the corresponding values obtained in conventional steady shear experiments [Tirtaatmadja *et al.* (1997a)]. Care was also taken to ensure that the oscillatory components remained in the linear region (σ_0 / γ_0 independent of σ_0) and that the magnitude of the phase angle δ was less than 90°.

III. RESULTS AND DISCUSSION

A. C20 HASE polymer—Comparison with complex hydrophobe polymer

The HASE polymers considered in this study contain *n*-alkyl hydrophobes of varying length and we will denote each polymer by its corresponding hydrophobe (e.g., the C20 HASE polymer bears *n*-alkyl moieties of length C_{20}). In the course of our discussion, we will contrast the response of these *n*-alkyl modified polymers with our previous data from

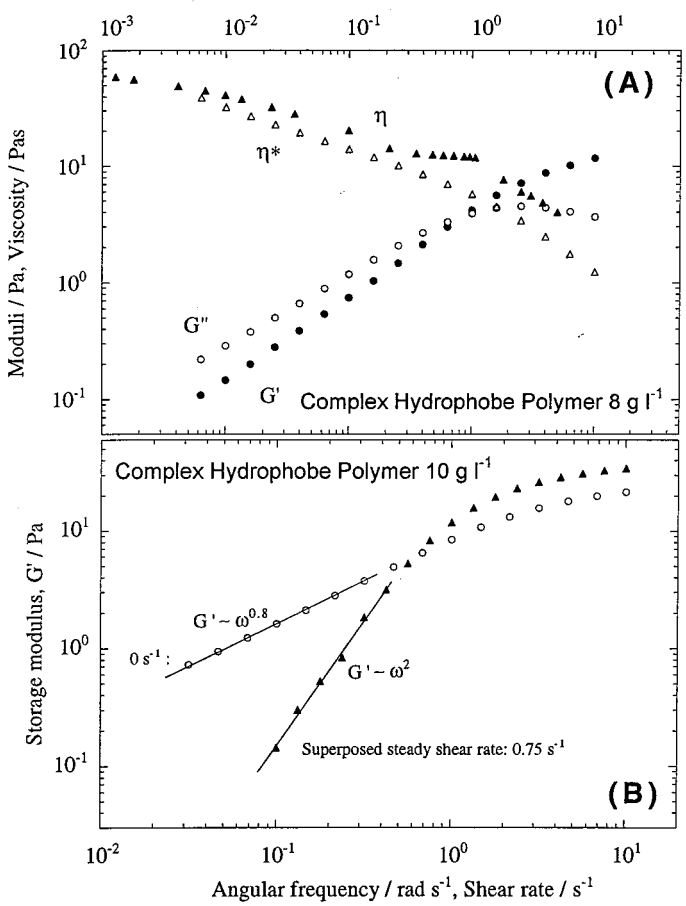

FIG. 2. Rheology of a HASE polymer based on a complex alkylaryl hydrophobe of high molar volume considered in a previous study [English *et al.* (1997)]. (A) Dynamic (G', G'', η^*) and steady shear data (η)—note the presence of a well-defined terminal region at low frequencies, indicative of a reversible network, and the structuring apparent at intermediate steady shear rates ($\eta > \eta^*$). (B) Shear-induced structuring as observed under parallel superposed steady/dynamic shear—note the increase in the plateau modulus. The shift of the terminal region to higher frequencies and appearance of second order behavior in G' is consistent with the loss of longer time modes of relaxation.

a HASE polymer bearing a small number of alkylaryl hydrophobes of high molar volume [English *et al.* (1997)]. In order to provide a basis for comparison, we first summarize in Fig. 2 the essential features of the rheology of this ''complex hydrophobe HASE polymer'' from our earlier study. Data are shown for a polymer solution of 8 $g\,l^{-1}$ and under several modes of deformation. We will refer to this data frequently in the rest of the paper.

We can now begin to analyze the rheology of typical *n*-alkyl HASE polymers, such as the C20 polymer. The variation in steady shear viscosity as a function of the applied shear stress for solutions of the C20 HASE polymer in aqueous alkaline media is depicted in Fig. 3. The most notable feature in the steady-shear response of the C20 polymer is the progressive increase in viscosity as the applied shear stress is reduced, so that there is no Newtonian plateau ($\eta \rightarrow \eta_0$) at low stresses. Indeed, the data almost suggest the presence of an apparent yield stress. Note that at such low stresses, we resorted to creep

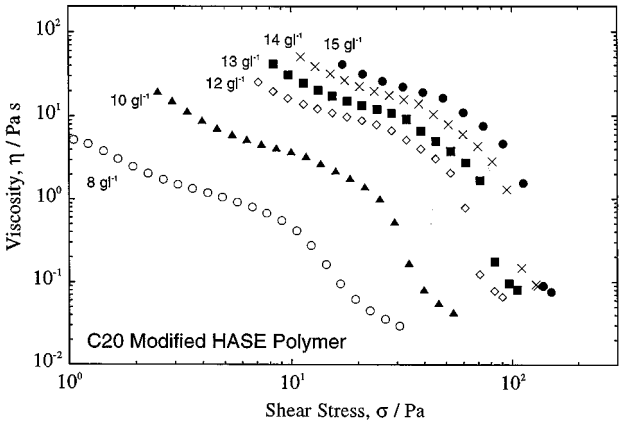

FIG. 3. Steady shear data for the C20 HASE polymer in aqueous alkaline media–steady shear viscosity as a function of imposed shear stress.

experiments to obtain our viscosity data. We found that very long times were required to reach a steady state (several hours at higher polymer concentrations) and the corresponding shear rates were in the region of 10^{-4}–$10^{-6}\,s^{-1}$. This indicated very high values of the viscosities ($> 10^4$ Pa s) for each sample at such low stresses. We have not shown these viscosities in Fig. 3 because there was considerable scatter in the data. Moreover, a constant equilibrium strain could not be attained within the duration of the creep experiments, even at the lowest applied stresses available experimentally. Thus, it was impossible to verify whether the samples possess a true yield stress. However, the incipient upturns in the viscosity at low stresses are reproducible on different measuring geometries and we are satisfied that wall slip effects are insignificant. We interpret these data in terms of a highly structured fluid having a low-shear viscosity of very high magnitude. Note that in contrast, solutions of the complex hydrophobe polymer [Fig. 2(A)] gave rise to a finite zero-shear viscosity over the range of polymer concentrations studied (see also Fig. 2 in our previous paper).

The structured nature of the C20 polymer solutions is clearly shown by the oscillatory shear data in Fig. 4, which depicts the frequency dependence of G' and G'' at several polymer concentrations. We note that the storage G' and loss G'' moduli are similar in magnitude over the range of concentrations. At the higher concentrations G' slightly dominates G'' over the entire range of frequencies, whereas at lower polymer concentrations ($c = 7\ gl^{-1}$) elastic modes of deformation become less dominant and G'' begins to exceed G'. Additionally, the moduli appear to be only weakly dependent on frequency across the entire range of experimentally accessible time scales. An interesting aspect of the data in Fig. 4 is that G' and G'' appear to show a similar frequency dependence, irrespective of polymer concentration. Thus, over the frequency range studied, the approximate scaling relationship $G', G'' \sim \omega^{0.4}$ is found to be valid. We can interpret the dynamic response in terms of a structured system that shows significantly elastic behavior over all timescales. Once again, we contrast this response with that of the complex hydrophobe polymer (Fig. 2) which showed a noticeably more viscous behavior at long timescales ($G'' > G'$ at low frequencies, with $G' \sim \omega^{0.8}$).

Selected viscosity data for C20 HASE polymer solutions are plotted as a function of shear rate in Fig. 5. In the same plot we show dynamic data for the corresponding systems in the form of $\eta^*(\omega)$. We note that the complex viscosity η^* follows the steady-

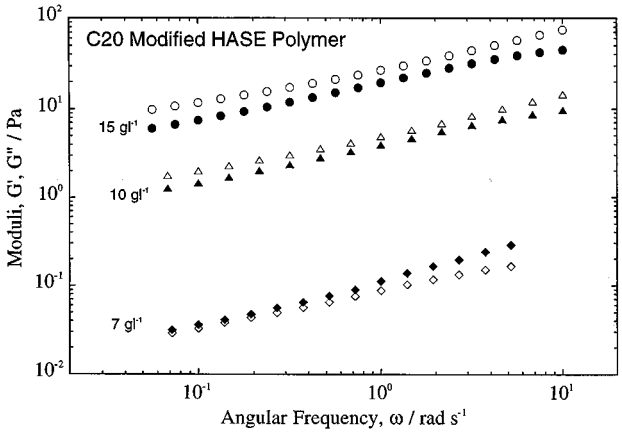

FIG. 4. Dynamic data for C20 HASE polymer systems–dynamic moduli as a function of angular frequency (filled symbols: G'', open symbols: G'). Note the weak frequency dependence of the material functions and the absence of a well-defined terminal region.

shear viscosity η quite closely at low polymer concentrations and high rates of deformation. This suggests that the Cox–Merz rule equating η and η^* is obeyed under these conditions. In contrast, the complex hydrophobe polymer showed anomalous deviations from the Cox–Merz rule, characterized by the relationship $\eta(\dot{\gamma}) > \eta^*(\omega)$ [Fig. 2(A)]. This unusual behavior was ascribed to shear-induced structuring in these polymer solutions at intermediate shear rates [English *et al.* (1997)].

We have also characterized the response of C20 HASE polymer solutions under large oscillatory deformations. Figure 6 shows the storage modulus G' as a function of stress amplitude, for a range of polymer concentrations. Again we are unable to discern any significant shear-induced structuring in these systems. In the case of the complex hydrophobe polymer, there was considerable strain hardening in G' at the onset of nonlinearity, for all concentrations studied [Fig. 4 in English *et al.* (1997)]. Here, a more typical

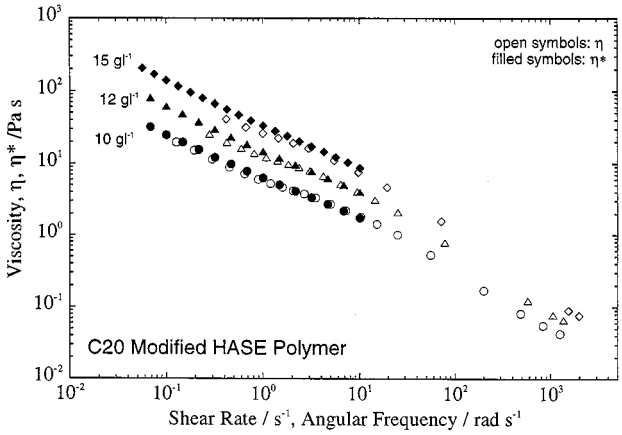

FIG. 5. Comparison of the steady shear (η) and dynamic (η^*) response of the C20 HASE polymer in aqueous media.

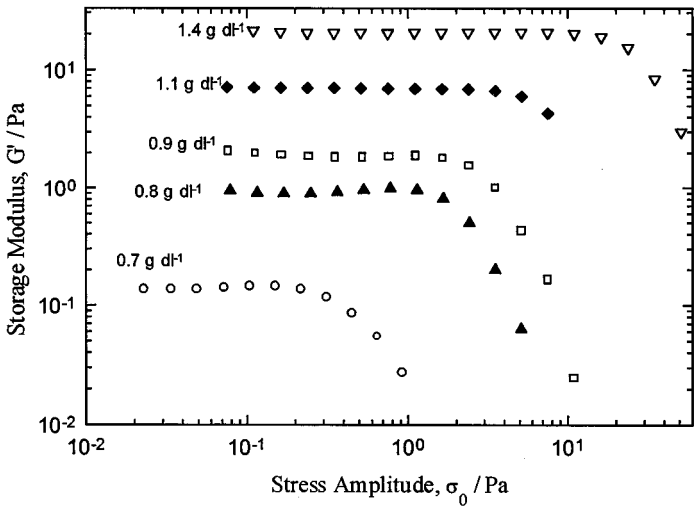

FIG. 6. Response of C20 HASE polymer systems under large amplitude oscillatory shear–storage modulus G' as a functional of increasing stress amplitude.

monotonic decrease in G' at high stress amplitudes is seen. There is perhaps a slight strain hardening at the lowest polymer concentrations [$c = 0.7-0.8\,\mathrm{g\,dl^{-1}}$].

A significant aspect of our previous work was the use of parallel-superposed steady/dynamic shear to characterize the shear-dependent microstructure of associative polymer systems. For the case of the complex hydrophobe polymer, we observed an increase in the plateau modulus at high frequencies, due to shear-induced structuring [Fig. 2(B)]. We now employ this technique for the C20 HASE polymer solutions under investigation. Data representing the frequency dependence of the storage modulus, obtained at different parallel-superposed shear rates are shown in Fig. 7(A). At the lowest rates of shear (0.035 $\mathrm{s^{-1}}$) the storage modulus G' is seen to follow the same weak frequency dependence as in the conventional dynamic experiment (Fig. 4). This is indicative of the microstructure being able to rearrange within the timescale of the superposed deformation. As the superposed rate of shear is increased, we see a pronounced decrease in G' at low frequencies, with the resultant G' scaling as ω^2. Thus a transition from a structured system to liquid-like behavior occurs on application of shear, and this transition is shifted to higher frequencies as the superposed deformation rate is increased. Such behavior has been widely interpreted as a truncation of the relaxation spectrum—modes of relaxation operating over longer times being lost due to the action of shear [Ferry (1980)].

The effects of superposed steady shear may also be represented in terms of the phase angle δ. While G' shows a catastrophic decrease, δ rises correspondingly to a value of 90° at low frequencies [Fig. 7(B)]. This again provides a useful means of pinpointing the effects of shear on the microstructure. There have been several attempts to characterize the relationship between the characteristic frequency ω_0 at which $\delta = 90°$ (i.e., $G' = 0$) and the superposed shear rate $\dot{\gamma}_m$. Following a comprehensive study of entangled polymer solutions, Booij (1966) proposed the following relationship:

$$\omega_0 = 0.5\dot{\gamma}_m. \tag{3}$$

Subsequent work by MacDonald (1973) found that a power law relationship of the form shown below was universally applicable in describing the response of polymeric systems:

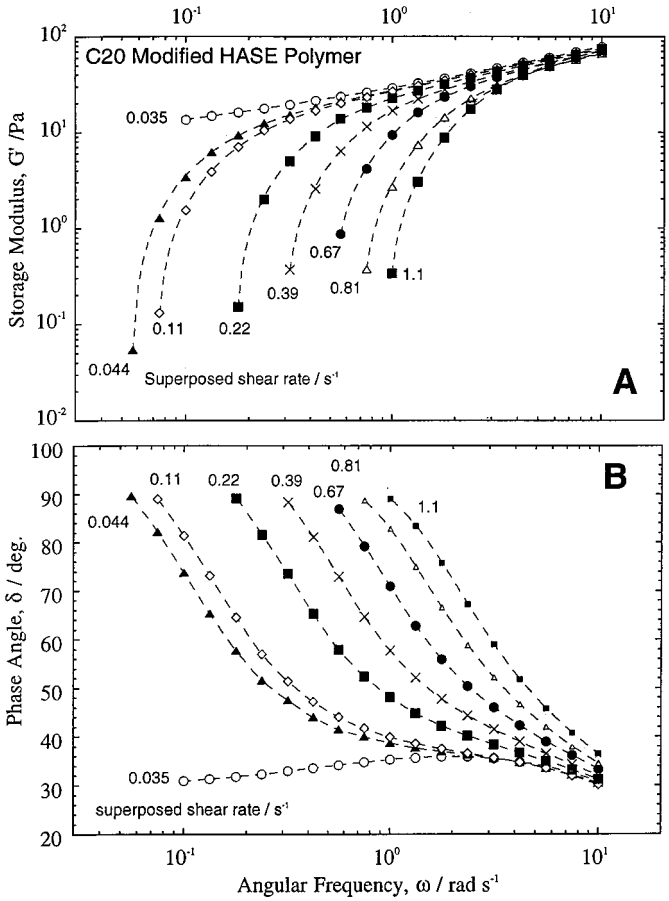

FIG. 7. Response of the C20 HASE polymer ($c = 15\ \mathrm{gl}^{-1}$) in parallel-superposed steady/dynamic shear. Data for (A) Storage modulus (G') and (B) phase angle (δ). Note the appearance of a terminal region in G', the onset of which progressively shifts to higher frequencies, as the magnitude of the superposed steady shear rate is increased.

$$\omega_0 = a(\dot{\gamma}_m)^b. \tag{4}$$

The above approach was later applied by Lapasin *et al.* (1992) to the solution rheology of both disordered and helical polysaccharides. A plot of ω_0 as a function of the superposed steady shear rate $\dot{\gamma}_m$ is shown in Fig. 8 for our system. The response of the C20 HASE polymer is observed to fit Eq. (4) very well, with an exponent $b \approx 0.8$. Further discussion of the effects of superposed steady/dynamic shear on *n*-alkyl HASE polymers can be found in the work of Tirtaatmadja *et al.* (1997a, b) who examined polymers of identical constitution to those considered here.

We have thus seen a number of striking differences between the rheology of the C20 polymer and the complex hydrophobe polymer considered in our previous work. We will presently discuss how we can account for these differences in rheological behavior on the basis of the microstructures existing in these systems, which in turn reflect the molecular architecture of the polymer chains. But first we will consider the effects of hydrophobe chain length in more detail—both under dilute and nondilute solution conditions.

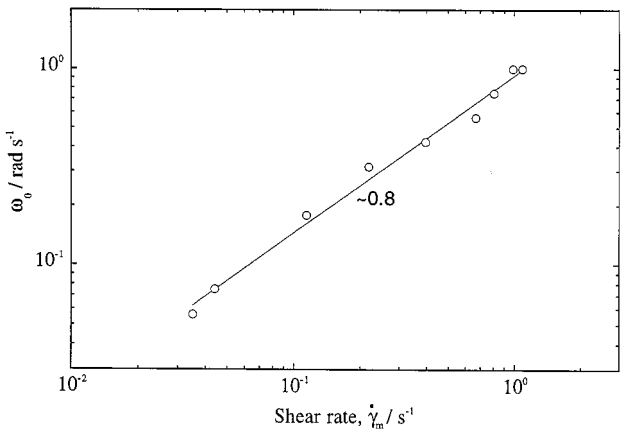

FIG. 8. Plot of the critical frequency ω_0 at which the phase angle δ becomes equal to 90°($G' = 0$), as a function of the superposed steady shear rate, for the C20 HASE polymer ($c = 15\,\mathrm{gl}^{-1}$).

B. Effect of hydrophobe size

We present in Figs. 9(A) and 9(B) the steady shear rheology (η vs σ) of C8 and C16 HASE polymer solutions over a range of concentrations. In all cases, we see a shear thinning behavior very different from that observed for solutions of the complex hydrophobe polymer [Fig. 2(A); also English *et al.*, 1997]. These data taken together with that of the C20 HASE polymer, allow us to examine the effect of hydrophobe size. The steady shear responses of the various *n*-alkyl HASE polymers at a polymer concentration of 10 gl^{-1} are compared in Fig. 10. We find that there is a progressive increase in viscosity building as the size of the hydrophobe is increased, in addition to an accentuation of non-Newtonian behavior. While the control polymer is practically Newtonian, shear thinning becomes more pronounced as the size of the hydrophobes increases.

The linear viscoelastic response of C8, C16, and C20 HASE polymers at a constant polymer concentration of 10 gl^{-1} are compared in Fig. 11. Here again, there are no major qualitative differences in the dynamic response with varying hydrophobe size, except that as we progress to longer *n*-alkyl chains, the magnitude of the storage modulus G' begins to exceed that of the loss modulus G'' (compare C20 and C8). Still the effect of hydrophobe size is largely similar to that of polymer concentration for a given hydrophobe (compare Figs. 4 and 11). In other words, regardless of the polymer concentration or hydrophobe size, the G' and G'' plots maintain the same weak dependence on frequency (approximately $\sim \omega^{0.4}$) over the entire accessible range of frequencies. The moduli increase with hydrophobe size as well as with polymer concentration.

The nature of the dynamic response of our systems suggests that it should be possible to scale the storage modulus (G') curves, to give master curves independent of concentration. However, the scaling factors for G' are indeed dependent on hydrophobe size. We illustrate this by showing the concentration dependence of G' at a constant angular frequency of 1.0 $\mathrm{rad\,s}^{-1}$ in Fig. 12 for the three different *n*-alkyl HASE polymers. Each of the polymers shows a power law relationship of the form $G' \sim c^n$, with the power law exponent n increasing with increasing hydrophobe size. We can then use the exponents obtained herein to scale G' curves, as shown in Fig. 13. Here we show a reduced modulus scaled with the appropriate concentration-dependent factor, plotted against frequency. We find that the data reduce to a master curve for each polymer. Moreover, these

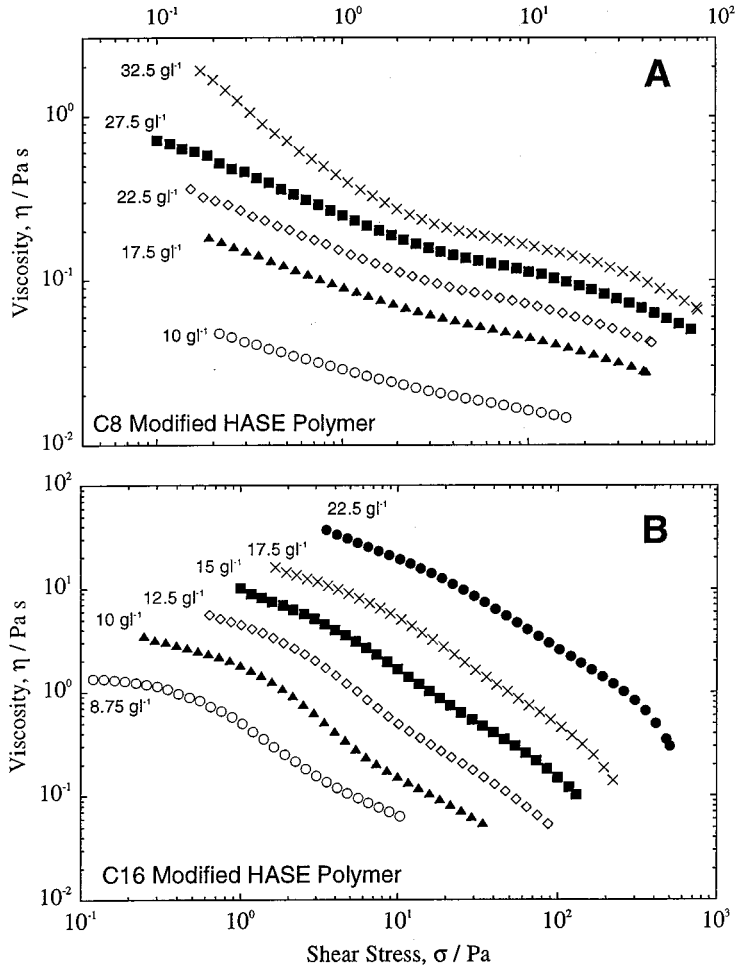

FIG. 9. Steady shear data–viscosity as a function of imposed shear stress—for (A) C8 HASE polymer systems and (B) C16 HASE polymer systems.

master curves are approximately parallel to each other, suggesting that the response of the three polymers is qualitatively identical, although the modulus level increases with increasing hydrophobe size. The microstructural significance of the above data analysis is discussed presently. From a practical standpoint, Figs. 12 and 13 indicate the superior thickening efficacy of HASE polymers containing longer *n*-alkyl hydrophobes.

It is now useful to consider the dilute solution behavior of *n*-alkyl HASE polymers in further detail, with a view to gaining further insight into the microstructure of alkali soluble/swellable systems. Viscometric data are presented in the form of the customary Huggins plot of (η_{sp}/c) vs c in Fig. 14. Linear regression analysis of these data allowed the corresponding intrinsic viscosities to be ascertained according to

$$\frac{\eta_{sp}}{c} = [\eta] + k'[\eta]^2 c. \tag{5}$$

The values of $[\eta]$ and k' calculated in this manner are summarized in Table III. The effect of hydrophobic modification is clearly shown as a decrease in $[\eta]$ as the size of the

TABLE III. Viscosities and Huggins coefficients for HASE polymers in aqueous alkaline media.

Polymer	$[\eta]$ dl g^{-1}	k'
Control	4.8	0.74
C8	4.3	0.68
C16	3.8	1.25
C20	1.3	12.6

hydrophobes is increased. Generally, the value of k' is also seen to increase as a function of the hydrophobe size, with the C20 polymer exhibiting an abnormally high value of k'. A similar effect has previously been reported for telechelic HEUR polymers in dilute solution [Jenkins *et al.* (1995)]. The results for $[\eta]$ might seem counterintuitive at first glance because the C20 polymer is shown to have the smallest $[\eta]$ among the three polymers. As we discuss in Sec. III C, these data are consistent with an interpretation of our systems as being similar to microgels.

C. Microstructure in *n*-alkyl HASE polymer systems

Before we discuss the microstructure in our systems, let us delve a little more into the molecular structure of these polymers. The *n*-alkyl HASE polymers were synthesized to contain $\sim$ 1.0% hydrophobic macromer on a molar basis. This translates to $\sim$ 16 hydrophobes per chain [Islam *et al.* (1999)], as opposed to roughly half this number in the case of the complex hydrophobe polymer characterized in our earlier paper [0.55% macromer on a molar basis]. Discounting differences in the constitution of the hydrophobes, the major difference between these two types of HASE polymers is the number of hydrophobes per chain. As we shall see, this crucial factor leads to profound microstructural variations between the two systems.

Let us now focus on the microstructure of HASE polymer latexes when ''solubilized'' in the presence of amines or alkali. On addition of alkali to a carboxylated acrylic latex, the latex particles are known to undergo swelling as the charge density on the chains is increased through ionization of the carboxy ($-COO^-$) functionalities [Verbrugge (1970); Quadrat and Snuparek (1990)]. In fact, particle swelling has been shown to be the pri-

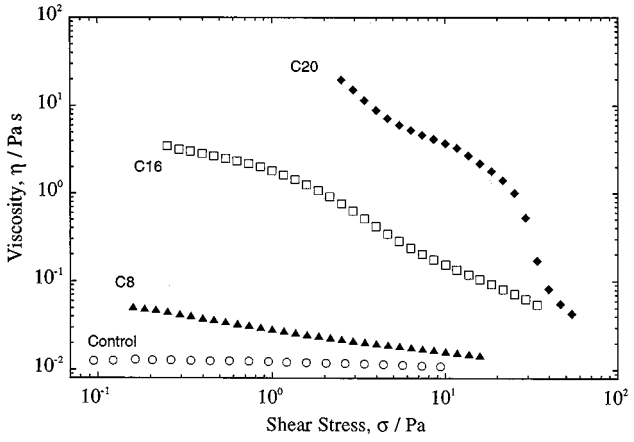

FIG. 10. Comparison of the steady shear response of the *n*-alkyl modified HASE polymers at $c = 10\,\mathrm{g\,l^{-1}}$, illustrating the influence of hydrophobe size on flow behavior. Data are also shown for a control polymer bearing no hydrophobes, at the same polymer concentration.

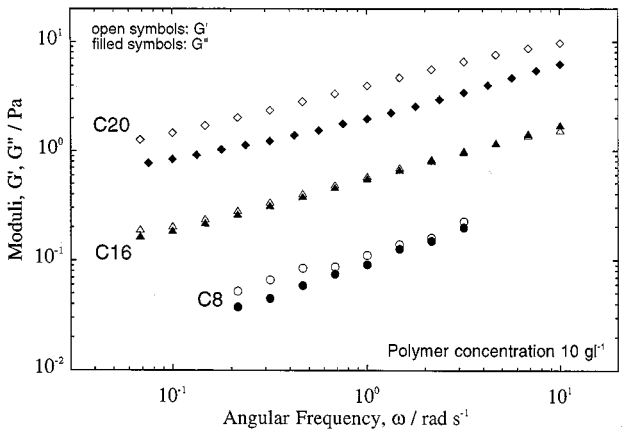

FIG. 11. Comparison of the linear viscoelastic response of the *n*-alkyl modified HASE polymers at $c = 10\,\mathrm{g l}^{-1}$, illustrating the influence of hydrophobe size on at-rest structure.

mary factor contributing to the viscosity rise on alkalinization of these systems. Ultimately, on sufficient increase in pH, the polymer chains can become solubilized, leading to an optically clear polymer solution. Potentiometric titration and light scattering studies previously presented for the C20 polymer have shown that the extent of viscosification correlates well with the degree of neutralization α of the carboxylate groups on the polymer backbone [Yekta *et al.* (1997); Horiuchi *et al.* (1998)]. From $\alpha = 0.05$ to 0.6 the pH remains constant at about 7. Microstructurally, significant changes occur with increasing degree of neutralization. The system is seen to become visually transparent at $\alpha = 0.2$, passing through a regime of time dependent swelling, to particle disintegration at $\alpha = 0.4$. When complete neutralization is attained ($\alpha = 1.0$) further addition of alkali leads to a rapid increase in pH and viscosification of the system.

However, the attainment of a visually transparent appearance on addition of alkali is not necessarily indicative of a transition to a ''true'' solution. As Verbrugge (1970) has pointed out, optical clarity could equally imply a true solution, swollen particles, or a

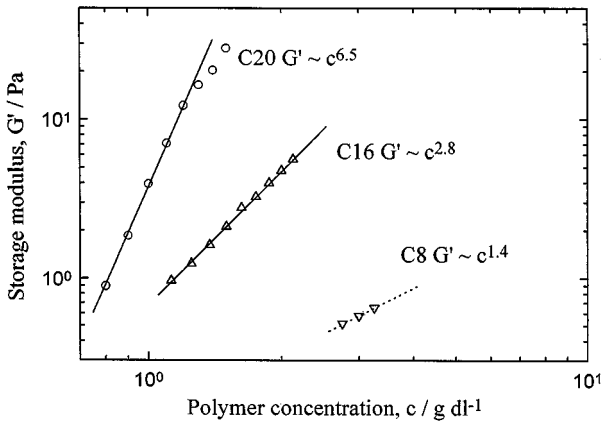

FIG. 12. Scaling of the storage modulus (at a constant frequency of 1 rad/s) with polymer concentration for each of the *n*-alkyl modified HASE polymers in aqueous media.

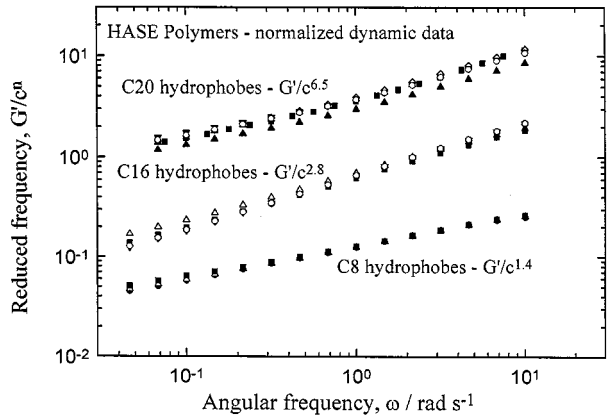

FIG. 13. Reduced storage modulus (G'/c^n) as a function of frequency for each of the *n*-alkyl HASE polymer systems. Note that the data reduces to a concentration-independent master curve for each polymer.

mixture of both. This is because the difference in refractive index between highly swollen particles and the medium would be small, so that the system would appear visually transparent. The degree of latex particle swelling/dissolution cannot be easily resolved by light scattering either. It is known from previous studies that complete solubilization occurs when the carboxylic content in the polymer is high (in excess of 55 mol%) [Quadrat and Snuparek (1990)]. At lower fractions of carboxylated comonomer, dissolution of the latex particles may be less developed, particularly in cases where the polymer has a high T_g or contains large proportions of hydrophobic monomers. For instance, in the presence of a large number of hydrophobes, particle dissolution may be hindered by hydrophobic associations within the swollen particle.

In the case of the HASE polymers considered here, little information relating the degree of hydrophobic modification (hydrophobe size and number) to the extent of particle swelling/solubilization has been ascertained until this point. We can however examine whether the rheological data presented herein is consistent with either of the conflict-

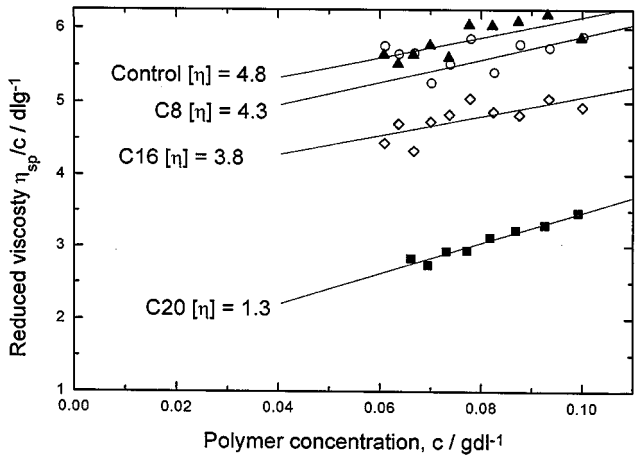

FIG. 14. Huggins plot for each of the *n*-alkyl polymers, together with equivalent data for a control polymer containing no hydrophobic modification.

ing hypotheses (solubilized chains versus swollen particles). In this context, we draw attention to the numerous parallels between our results and that for covalently crosslinked acrylic microgels (''carbopols''), which are widely used as thickeners in various applications [Nae and Reichert (1992); Ketz *et al.* (1988)]. The microgel systems consist of lightly crosslinked acrylic particles, which also swell dramatically on adding alkali. Beyond an ''overlap concentration,'' the microgel particles become close packed and space filling, whereupon the viscosity of the system sharply increases. Thereafter, the systems exhibit a low shear viscosity of high magnitude, as well as significant shear thinning under steady shear. Under oscillatory shear, a weak power-law dependence of G' and G'' (both scaling as $\sim \omega^{0.2-0.4}$) is found over the entire frequency range. The moduli for microgel systems can also be reduced to master curves independent of concentration by scaling with c^n [Ketz *et al.* (1988)].

The above features in the rheology of concentrated microgels bear a striking resemblance to the rheology of *n*-alkyl HASE polymers reported here. These similarities evidently suggest a correspondence between the microstructures in the two systems. We can therefore envisage our HASE latex particles swelling in the presence of alkali, with the hydrophobic associations preventing complete particle dissolution. As the pH is increased, the latex particles are envisaged as breaking down into smaller aggregates, as demonstrated previously by Snuparek and co-workers (1993). Thus, it is both the number and molar volume of the hydrophobic groups [Hildebrand and Scott (1964)] which ultimately dictates the structure of the polymer aggregates formed on alkalinization of the parent latex. At high concentrations, these supramolecular aggregates would become close packed, leading to a microstructure akin to that in crosslinked microgels. Since the particles fill the volume, an applied (low-amplitude) oscillatory stress is never allowed to relax completely, which is why we do not observe a terminal region ($G'' > G'$, with highly frequency dependent moduli) for our systems. At the same time, the particles are not connected by rigid bonds, so that the response is not completely elastic. Instead, the microstructure relaxes slowly, possibly by the internal deformation of individual particles. The compressibility (''softness'') of the particles is then the parameter that mediates the rigidity (moduli) of the close-packed network structure at small deformations [Ketz *et al.* (1988); Evans and Lips (1990); Carnali and Naser (1992)].

Based on the above microstructural hypothesis, we can explain the rheological data reported herein. We first consider the intrinsic viscosity data (Fig. 14) which shows that $[\eta]$ decreases with increasing hydrophobe size. Assuming that the data correspond to dilute dispersions of *n*-alkyl HASE polymer aggregates formed on alkalinization, $[\eta]$ will correlate with the hydrodynamic size of the particles and will reflect their swollen volume [Carnali and Naser (1992)]. We can therefore conclude from our data that particle swelling decreases as the length of the *n*-alkyl hydrophobes increases. This result is consistent, if we consider swelling of the aggregates to be restricted by hydrophobic associations, and the driving force behind association to increase with the molar volume of the hydrophobes [Hildebrand and Scott (1964)]. In other words, the C20 polymer aggregates are smaller and less compressible than say the C8 aggregates, owing to more extensive hydrophobic associations. Consequently, the C8 latex swells more than the C20 latex, and can hence be considered a softer (more compressible) particle due to its higher solvent content.

Figure 14 also suggests that the rheology of *n*-alkyl HASE polymer dispersions will show different trends above and below the overlap (space-filling) concentration. This overlap concentration can be estimated to be $\approx 1/[\eta]$ [Carnali and Naser (1992)]. Until this point, the specific viscosities of the systems will follow the order C8 $>$ C16 $>$ C20, consistent with the more swollen C8 aggregates occupying a larger

volume fraction. Moreover, particles that swell strongly will reach the space-filling condition at a lower concentration ($\equiv c^*$) than their less swollen analogs. Beyond the overlap concentration, however, the rheology will be dictated by the deformability of the particles. (All the concentrations reported in Figs. 3–13 correspond to the latter regime.) Thus, since the C20 particles are the most rigid, their close-packed network will deform the least—which explains why the level of modulus (G') is highest for C20 (Fig. 13). Likewise increasing the concentration for a given *n*-alkyl HASE polymer implies a transition to a system of more rigid (less swollen) particles which exhibits a higher dynamic modulus.

On application of shear, the particles can slide past each other with increasing ease, which explains the drastic shear thinning in our systems. This mechanism has been considered in detail by Ketz *et al.* (1988). Here, slippage between particles is considered to occur once a critical macroscopic strain is attained. For a two dimensional lattice of monodisperse, interpenetrable spheres, this critical strain is calculated to be 0.57, from purely geometrical considerations. In three dimensions, the magnitude of the critical strain is less. Polydispersity and interpenetration of the microgel particles also act to reduce the critical strain. In the case of the C20 polymer, in oscillatory shear, the onset of nonlinearity occurs at around $\gamma_0 = 0.3$, across the concentration regime considered, which is reasonably consistent with this model. Furthermore, if no interpenetration of the particles occurs, flow at constant stress is predicted (i.e., $\eta \sim \dot{\gamma}^{-1}$). In the case of the C20 polymer, an exponent of ~ -0.9 is seen, in the region where shear thinning is most pronounced. Such behavior may also suggest some interpenetration of the microgel particles. We can also extend these arguments to explain our results from superposed steady/oscillatory shear. The overall connectivity of the close-packed arrangement is expected to be lost under shear as particles can deform and slide past each other—we therefore begin to see more liquid-like behavior ($G' \sim \omega^2$ at long timescales).

A variety of other systems, in addition to microgels and HASE polymers, exhibit similar rheological behavior as above [Sollich *et al.* (1997)]. These include foams, emulsions, and lamellar ''onion phases.'' The most notable feature in the rheology of these systems is the weak power-law behavior of G' and G'', with the two moduli in nearly constant ratio. From a microstructural perspective, the common theme to these diverse materials is the presence of a ''cellular lattice'' formed by nonrigid particles or droplets or beads, extending throughout the sample volume in a close-packed arrangement.

We can also begin to comprehend why there are considerable differences between the rheology of the *n*-alkyl HASE polymers and the complex hydrophobe HASE polymer that we considered previously. In the latter case, we observed a terminal region in our frequency spectra (Fig. 2), i.e., the stresses relaxed at long timescales in these systems, much like in a conventional polymer solution. Furthermore, we observed shear-induced transitions under steady and oscillatory shear, both of which are consistent with chain elongation under shear. These results suggest that the complex hydrophobe HASE polymer indeed forms an associative polymer solution, with dissolution of the latex particles being essentially complete at high pH. This is in contrast to the *n*-alkyl HASE polymers which are considered to form swollen aggregates on alkalinization. In order to confirm these microstructural interpretations, we will need to resort to techniques that allow a direct visualization of the microstructure in the nondilute regime. The methods of cryo-TEM or freeze-fracture TEM would be particularly useful in this respect and the use of the latter technique will be the subject of a future study. Advancement of our understanding of these industrially important rheology modifiers will also require further experimental studies on systems of well-defined molecular architectures.

IV. CONCLUSIONS

Our study indicates that it is possible to tailor the rheology of associative polymer systems, largely through manipulation of the mean number of hydrophobes per chain. When the number of hydrophobes is small, solubilization of the latex by alkali is complete and the solution rheology is then dictated by associative interactions between the hydrophones and physical entanglements of the chains. On the other hand, polymer latexes bearing a large number of hydrophobes resist dissolution and instead form a close-packed array of swollen aggregates. This microstructure resembles that present in concentrated acrylic microgels (e.g., carbopols) and, correspondingly, the dynamic rheology reveals a slow but steady relaxation extending to long timescales. Interactions between hydrophobes within each particle dictate the extent of particle swelling, and hence the deformability of the particles, and this in turn determines the level of modulus for the system.

ACKNOWLEDGMENTS

The authors would like to acknowledge the services of Garland Fussell and Jeffrey Giles in performing the intrinsic viscosity measurements reported in this study as well as for assisting with the rheological experiments.

References

Annable, T. R., R. Buscall, R. Ettelaie, and D. Whittlestone, ''The Rheology of Solutions of Associating Polymers: Comparison of Experimental Behavior with Transient Network Theory,'' J. Rheol. **37**, 695–726 (1993).

Booij, H. C., ''Influence of Superimposed Steady Shear Flow on the Dynamic Properties of Non-Newtonian Fluids,'' Rheol. Acta **5**, 215–221 (1966).

Borisov, O. V. and A. Halperin, ''Micelles of Polysoaps,'' Langmuir **11**, 2911–2919 (1995).

Borisov, O. V. and A. Halperin, ''Micelles of Polysoaps: The Role of Bridging Interactions,'' Macromolecules **29**, 2612–2617 (1996a).

Borisov, O. V. and A. Halperin, ''On the Elasticity of Polysoaps—The Effects of Secondary Structure,'' Europhys. Lett. **34**, 657–662 (1996b).

Branham, K. D., H. S. Snowden, and C. L. McCormick, ''Water-Soluble Copolymers. 64. Effects of pH and Composition on Associative Properties of Amphililic Acrylamide/Acrylic Acid Terpolymers,'' Macromolecules **29**, 254–262 (1996).

Bromberg, L., ''Scaling of Rheological Properties of Hydrogels from Associating Polymers,'' Macromolecules **31**, 6148–6156 (1998).

Carnali, J. O. and M. S. Naser, ''The Use of Dilute Solution Viscometry to Characterize the Network Properties of Carbopol Microgels,'' Colloid Polym. Sci. **270**, 183–193 (1992).

English, R. J., H. S. Gulati, R. D. Jenkins, and S. A. Khan, ''Solution Rheology of a Hydrophobically Modified Alkali-Soluble Associative Polymer,'' J. Rheol. **41**, 427–444 (1997).

Evans, I. D. and A. Lips, ''Concentration Dependence of the Linear Elastic Behavior of Model Microgel Dispersions,'' J. Chem. Soc., Faraday Trans. **86**, 3413–3417 (1990).

Ferry J. D., *Viscoelastic Properties of Polymers*, 3rd ed. (Wiley, New York, 1980).

Groot, R. D. and W. G. M. Agterof, ''Dynamic Viscoelastic Modulus of Associative Polymer Networks: Off-Lattice Simulations, Theory and Comparison to Experiments,'' Macromolecules **28**, 6284–6295 (1995).

Guo, L., K. C. Tam, and R. D. Jenkins, ''Effects of Salt on the Intrinsic Viscosity of Model Alkali-Soluble Associative Polymers,'' Macromol. Chem. Phys. **199**, 1175–1184 (1998).

Hildebrand J. H. and R. L. Scott, *The Solubility of Non-Electrolytes* (Dover, New York, 1964).

Horiuchi, K., Y. Rharbi, A. Yekta, M. A. Winnik, R. D. Jenkins, and D. R. Bassett, ''Dissolution Behavior in Water of a Model Hydrophobic Alkali-Swellable Emulsion (HASE) Polymer with $C_{20}H_{41}$ Groups,'' Can. J. Chem. **76**, 1779–1787 (1998).

Islam, M. F., R. D. Jenkins, H. D. Ou-Yang, and D. R. Bassett, ''Single Chain Characterization of Hydrophobically Modified Polyelectrolytes using Cyclodextrin/Hydrophobe Complexation,'' Proceedings International Conference on Associative Polymers, Fontevrand, France, 1997.

Islam, M. F., R. D. Jenkins, H. D. Ou-Yang, and D. R. Bassett, ''Single Chain Characterization of Hydrophobically Modified Polyelectrolytes using Cyclodextrin/Hydrophobe Complexation,'' Macromolecules (in press, 1999).

Jenkins R. D., ''The Fundamental Thickening Mechanism of Associative Polymers in Latex Systems—A Rheological Study,'' Ph.D. thesis, Lehigh University, 1990.

Jenkins R. D., D. R. Bassett, and G. D. Shay, ''Polymers Containing Macromonomers,'' United States Patent 5,292,843 (1994).

Jenkins, R. D., D. R. Bassett, C. A. Silebi, and M. S. El-Aasser, ''Synthesis and Characterization of Model Associative Polymers,'' J. Appl. Polym. Sci. **58**, 209–230 (1995).

Jenkins R. D., L. M. DeLong, and D. R. Bassett, ''Influence of Alkali-Soluble Associative Emulsion Polymer Architecture on Rheology,'' in *Hydrophilic Polymers: Performance with Environmental Acceptance*, edited by J. E. Glass (ACS Advances in Chemistry Series No. 248 American Chemical Society, Washington, DC, 1996).

Jenkins R. D., C. A. Silebi, and M. S. El-Aasser, ''Steady Shear and Linear Viscoelastic Properties of Model Associative Polymer Solutions,'' in *Polymers as Rheology Modifiers*, edited by J. E. Glass (ACS Symposium Series No. 462 American Chemical Society, Washington, DC, 1991).

Ketz, R. J., R. K. Prud'homme, and W. W. Graessley, ''Rheology of Concentrated Microgel Solutions,'' Rheol. Acta **27**, 531–539 (1988).

Kumacheva, E., Y. Rharbi, M. A. Winnik, L. Guo, K. C. Tam, and R. D. Jenkins, ''Fluorescence Studies of an Alkali Swellable Associative Polymer in Aqueous Solution,'' Langmuir **13**, 182–186 (1997).

Lapasin, R., S. Pricl, and P. Tracanelli, ''Different Behaviours of Concentrated Polysaccharide Systems in Large Amplitude Oscillating Shear Fields,'' Rheol. Acta **31**, 374–380 (1992).

Leibler, L., M. Rubinstein, and R. H. Colby, ''Dynamics of Reversible Networks,'' Macromolecules **24**, 4701–4707 (1991).

Macdonald, I. F., ''Parallel Superposition of Simple Shearing and Small Amplitude Oscillatory Motions,'' Trans. Soc. Rheol. **17**, 537–555 (1973).

Nae, H. N. and W. W. Reichert, ''Rheological Properties of Lightly Crosslinked Carboxy Copolymers in Aqueous Solutions,'' Rheol. Acta **31**, 351–360 (1992).

Quadrat, O. and J. Snuparek, ''Structure and Flow Properties of Lattices Containing Carboxylic Groups,'' Prog. Org. Coat. **18**, 207–228 (1990).

Rubinstein, M. and A. V. Dobrynin, ''Solutions of Associative Polymers,'' Trends Polym. Sci. **5**, 181–186 (1997).

Rubinstein, M., and A. N. Semenov, ''Thermoreversible Gelation in Solutions of Associating Polymers. Linear Dynamics,'' Macromolecules **31**, 1386–1397 (1998).

Semenov, A. N., J.-F. Joanny, and A. R. Khokhlov, ''Associating Polymers: Equilibrium and Linear Viscoelasticity,'' Macromolecules **28**, 1066–1075 (1995).

Shay, G. D., ''Alkali-Swellable and Alkali-Soluble Thickener Technology'' in ''Polymers in Aqueous Media—Performance Through Association,'' edited by J. E. Glass, Adv. Chem. Ser. **223**, 457–494 (1989).

Shay, G. D. and A. F. Rich, ''Urethane-Functional Alkali-Soluble Associative Latex Thickeners,'' J. Coat. Technol. **58**, 43–53 (1986).

Snuparek, J., P. Bradna, L. Mrkvickova, F. Lednicky, and O. Quadrat, ''Effect of Coagulative Mechanism of Particle Growth on the Structural Heterogeneity of Ethyl Acrylate-Methacrylic Acid Copolymer Latex Particles,'' Collect. Czech. Chem. Commun. **58**, 2451–2457 (1993).

Sollich, P., F. Lequeux, P. Hebraud, and M. E. Cates, ''Rheology of Soft Glassy Materials,'' Phys. Rev. Lett. **78**, 2020–2023 (1997).

Tam, K. C., R. D. Jenkins, M. A. Winnik, and D. R. Bassett, ''Structural Model of Hydrophobically Modified Urethane-Ethoxylate (HEUR) Associative Polymers in Shear Flows,'' Macromolecules **31**, 4149–4159 (1998).

Tanaka, F. and S. F. Edwards, ''Viscoelastic Properties of Physically Crosslinked Networks (Parts 1, 2 and 3),'' J. Non-Newtonian Fluid Mech. **43**, 247–309 (1992).

Tirtaatmadja, V., K. C. Tam, and R. D. Jenkins, ''Superposition of Oscillations on Steady Shear Flow for Investigating the Structure of Associative Polymers,'' Macromolecules **30**, 1426–1433 (1997a).

Tirtaatmadja, V., K. C. Tam, and R. D. Jenkins, ''Rheological Properties of Model Alkali-Soluble Associative (HASE) Polymers: Effect of Varying Hydrophobe Chain Length,'' Macromolecules **30**, 3271–3282 (1997b).

Tirtaatmadja, V., K. C. Tam, R. D. Jenkins, and D. R. Bassett, ''Stability of a Model Alkali-Soluble Associative Polymer in the Presence of a Weak and Strong Base,'' Colloid Polym. Sci. **277**, 276–281 (1999).

Verbrugge, C. J., ''Mechanism of Alkali Thickening of Acid-Containing Emulsion Polymers. I. Examination of Latexes by Means of Viscosity,'' J. Appl. Polym. Sci. **14**, 897–909 (1970).

Xu, B., A. Yekta, L. Li, Z. Masoumi, and M. A. Winnik, ''The Functionality of Associative Polymer Networks–The Association Behavior of HEUR Associative Polymers in Aqueous Solution,'' Colloids Surf., A **112**, 239–250 (1996).

Yekta A., H. Kazunaga, and M. A. Winnik, ''pH Dependence of Microstructural Transformations in HASE Polymers,'' Poster Presentation, International Conference on Associative Polymers, Fontevrand, France, 1997.